

Article

# Heterogeneous Catalytic Ozonation of p-Chlorobenzoic Acid in Aqueous Solution by FeMnOOH and PET

Savvina Psaltou<sup>1</sup>, Stylianos Stylianou<sup>1</sup>, Manasis Mitrakas<sup>2</sup>  and Anastasios Zouboulis<sup>1,\*</sup> 

<sup>1</sup> Division of Chemical Technology, Department of Chemistry, Aristotle University, 54124 Thessaloniki, Greece; psaltousavvina@gmail.com (S.P.); s.stylianou@gmail.com (S.S.)

<sup>2</sup> Department of Chemical Engineering, Aristotle University, 54124 Thessaloniki, Greece; manasis@eng.auth.gr

\* Correspondence: zouboulis@chem.auth.gr; Tel.: +30-231-0997794

Received: 21 May 2018; Accepted: 8 August 2018; Published: 20 August 2018



**Abstract:** The oxidation of p-chlorobenzoic acid (p-CBA), used as a typical-model refractory organic compound, in aqueous solutions during the heterogeneous catalytic ozonation treatment process by applying the hydrophilic tetravalent manganese ferrioxalate (TMFx), as well as modified hydrophobic TMFx and the polyethylene terephthalate (PET) as solid (powdered) catalysts was examined in this study. TMFx was hydrophobically modified by using trichloromethylsilane (TriCIMS) solutions in toluene at the concentration range 10–1000 mg/L. TMFx catalysts were characterized by the application of scanning electron microscopy (SEM), as well as by Brunauer-Emmet-Teller (BET) and surface charge density determinations. TMFx catalyst, which was modified by 50 mg/L trichloromethylsilane (TriCIMS) solution (TMFx-50), was found to present the higher adsorption capacity of studied organic compound (250 µg p-CBA/g) when compared with all the other investigated catalysts, which in turn resulted in the higher removal of p-CBA (>99%) by the subsequent application of ozonation, as compared to hydrophilic TMFx (96.5%) and to single ozonation (96%) applications. PET-catalyst concentration in the range 0.5–10 g/L led to almost total removal of p-CBA within 15 min of reaction/oxidation time at pH 7. Conclusively, the experimental results for both catalysts indicated that hydrophobicity and adsorption capacity are crucial steps for the process of heterogeneous catalytic ozonation of refractory organic compounds.

**Keywords:** heterogeneous catalytic ozonation; adsorption; iron-manganese oxy-hydroxide; p-chlorobenzoic acid; PET

## 1. Introduction

A variety of organic compounds, such as pharmaceuticals, personal care products, steroid hormones, and plasticizers, have been characterized as emerging contaminants [1,2]. These compounds are usually termed also as micropollutants, due to their low concentrations (pg/L to ng/L) in aquatic ecosystems [3]. Since conventional treatment processes are not suitable for the efficient mineralization/destruction of them, they tend to concentrate in environmental matrixes and can cause serious health problems, acting eventually as e.g., Endocrine Disruptive Compounds (EDCs) [4].

In recent years several Advanced Oxidation Processes (AOPs) have been commonly implemented for the efficient oxidation of these refractory, non-biodegradable compounds [5]. Among them, ozonation is considered to be the most commonly applied treatment process for the removal of such compounds, which may proceed either via the direct reaction of micropollutants with molecular ozone, or through the production of hydroxyl radicals (OH·) [6]. However, high ozonation efficiency may also present undesirable side effects, such as specific by-product formation, which can be as harmful

as the original pollutants to be treated [2]. The most common by-products can be aldehydes, alcohols, ketones, carboxylic acids, ethers, olefins, amines, and other aromatic compounds, which are generally very difficult to predict precisely [6]. For the elimination of side effects and to improve its oxidation efficiency, the ozonation process can be optimized through the presence of an appropriate catalyst (catalytic ozonation) [7].

Catalytic ozonation is also considered as an Advanced Oxidation Process and, as with all the other AOP processes, is usually based on the production of hydroxyl radicals [5,8], which are a very reactive oxidative species, because they present high reaction rate constants ( $10^6$ – $10^9$   $M^{-1}s^{-1}$ ) especially with organic compounds. However, in some cases solid reactions are responsible for the removal of the micropollutants [9,10]. Catalytic ozonation can be conceptually divided into two different processes, i.e., homogeneous and heterogeneous [7]. While the homogeneous process commonly requires the addition of certain chemical reagents and/or dissolved metal cations, such as  $H_2O_2$ , Fe, Zn etc., the heterogeneous catalytic ozonation combines the adsorptive properties of an appropriate solid (usually in granular form) catalyst with the high oxidation capacity of ozone, resulting either to the mineralization or modification of refractory organic compounds to carbon dioxide, inorganic acids or lower molecular compounds at ambient temperature [5]. A variety of materials have been examined as catalysts in this process, such as metal oxides [9,11–14], minerals [15] and activated carbon [10,16]. The choice of an efficient low-cost catalytic material diminishes the cost of treatment process. Therefore, many materials of the above groups (volcanic sand [17], iron and manganese-based materials [18,19]) are low cost and appear to be a promising approximation for catalytic ozonation.

p-chlorobenzoic acid (p-CBA) is an important intermediate in the production of various products, such as dyes, pesticides, and pharmaceuticals, which can be formed by the chlorination process, such as during the bio/degradation of polychlorinated biphenyls [20,21]. p-CBA ( $pK_a = 3.99$ ) reacts very slowly with ozone ( $k_{O_3/p-CBA} < 0.15$   $M^{-1}s^{-1}$ ), but has high reactivity with hydroxyl radicals ( $k_{OH\cdot/p-CBA} = 5 \times 10^9$   $M^{-1}s^{-1}$ ). Therefore, it has been characterized as an  $OH\cdot$ /probe compound, being used in relevant studies to prove if a catalyst can enhance the production of  $OH\cdot$  radicals [22,23].

The aim of this study was to study the contribution of adsorption capacity and hydrophobicity of certain catalysts for p-CBA degradation by the application of heterogeneous catalytic ozonation in aqueous solutions. For this purpose, the examined materials were the hydrophilic tetravalent manganese ferrioxhyte (TMFx, i.e.,  $FeMnOOH$ ), presenting high surface area and charge density, the (modified) hydrophobized TMFx and the hydrophobic polyethylene terephthalate (PET), showing different surface properties, which were related with their adsorption capacity for p-CBA and degradation efficiency.

Both materials have never been reported in the published literature as catalysts in the ozonation process. However, although TMFx has some textural similarities with other catalysts, such as  $FeOOH$  that has been used before for the removal of micropollutants [14,24], it incorporates a significant percentage ( $12.5 \pm 0.5$  wt %) of high oxidative Mn(IV). Moreover, TMFx presents significantly higher surface area and charge density in comparison to manganese oxide-based materials that were frequently employed in heterogeneous catalytic ozonation processes and showed great catalytic activity [12,25,26].

## 2. Materials and Methods

### 2.1. Materials and Reagents

The p-CBA (purity 99%, Cas No. 74-11-3) was obtained from Sigma-Aldrich (St. Louis, MO, USA). Except for the HPLC-grade phosphoric acid and acetonitrile, all other chemical agents used in this study were of analytical reagent grade. 100  $\mu$ M stock solution of this compound was prepared by the dissolution of 15.66 mg p-CBA in 1 L distilled water. In this study, distilled water was used to prepare all aqueous solutions. TMFx and PET were used as catalysts. PET (commercially available) had particle sizes smaller than 2 mm and TMFx had an average granular size lower than 0.63  $\mu$ m. Table 1 summarizes the main properties of TMFx catalyst.

**Table 1.** Main physicochemical characteristics of tetravalent manganese feroxyhyte (TMFx) [27].

Characteristics	Fe/Mnratio (wt %)	IEP	PZC	Surface Charge (mmol OH <sup>-</sup> /g)	Surface Charge (mmol H <sup>+</sup> /g)	S <sub>BET</sub> (m <sup>2</sup> /g)	Pore Volume (mL/g)	Pore Diameter (Å)
TMFx	41/12.7	7.5	3.4	3.24	0.13	85	0.12	29

wt %: weight percentage, IEP: Iso-Electric Point, PZC: Point of Zero Charge.

It can be noticed that this catalyst, when used in unmodified (hydrophilic) form, was found to present more negative sites (3.24 mmol OH<sup>-</sup> /g) on its surface, than positive (0.13 mmol H<sup>+</sup> /g).

### 2.2. Modification of TMFx Hydrophilicity

The method proposed by Stylianou et. al. [28] was implemented to increase the hydrophobicity of TMFx surface. 2 g of TMFx powder with size lower than 63 μm was immersed in 150 mL trichloro-methyl-silane (TriClMS) solution in toluene, with different concentrations (10, 50, 100, 250, 500 and 1000 mg/L). The suspension was agitated for 6 hat ambient temperature. After that the catalyst was separated by membrane filtration (0.45 μm), rinsed three times with toluene to remove the excess of TriClMS and dried at 100 °C for 1 h in vacuum oven. The resulting hydrophobically modified TMFx samples are abbreviated hereafter as TMFx-10, TMFx-50, TMFx-100, TMFx-250, TMFx-500 and TMFx-1000, respectively.

### 2.3. Adsorption Experiments

Adsorption experiments were performed in batch mode. The initial p-CBA concentration was 4 μM and the solution pH was adjusted to 7, by using the 0.005 M K<sub>2</sub>HPO<sub>4</sub>/KH<sub>2</sub>PO<sub>4</sub> buffer solution. For all these experiments the adsorption/contact time was 20 min. Subsequently, the water samples were filtered through a 0.45 μm membrane filter and the residual p-CBA concentration was determined.

The amount of adsorbed p-CBA (μg/g) was calculated based on the following equation, regarding sorption capacity—Equation (1):

$$q = \frac{[(C_o - C_e) \times V]}{W} \quad (1)$$

where  $q$  is the adsorption capacity (μg/g),  $C_o$  is the initial concentration of p-CBA (μg/L),  $C_e$  is the equilibrium/residual concentration (μg/L),  $V$  is the volume of the solution (L) and  $W$  is the dry weight of the respective catalysts (g).

### 2.4. Ozonation Procedures

Ozonation experiments were performed in a dark-colored vessel (250 mL) in batch mode, following the procedure suggested by Staehelin and Hoigne [29]. Ozone was generated using a corona discharged ozone generator with pure oxygen as the feed gas (Ozonia-Triogen, Model TOGC2A). The initial p-CBA concentration was 4 μM in 0.1 M K<sub>2</sub>HPO<sub>4</sub>/KH<sub>2</sub>PO<sub>4</sub>buffer solution to keep the pH value constant at 7 and the concentration of applied ozone dissolved in aqueous phase was 2 mg/L. The ozonation and the catalytic ozonation reaction/contact time was 15 min for all these experiments. Water samples were taken at reaction times 1, 3 and 15 min, filtered through a 0.45 μm membrane filter and the residual concentrations of ozone and p-CBA were determined. The oxidation reaction was stopped by the addition of an appropriate amount of indigo stock solution. Ozonation experiments did not influence the textural stability (specific surface area, porosity) and Point-of-Zero Charge (PZC) of the catalysts.

### 2.5. Analytical Methods

The concentration of p-CBA was determined by using the High-Performance Liquid Chromatography system (HPLC Thermo Fisher Scientific Inc., model of UV Spectrum UV2000, Waltham, MA, USA) at 254 nm, using a 4.6 mm × 250 mm reversed phase column (AGILENT, model Eclipse Plus C18, Santa Clara, CA, USA) and applying a 10 mM phosphoric acid and acetonitrile

(60:40 *v/v*) solution as the mobile phase. The detection limit was 0.025  $\mu\text{M}$  and the linear response in the range 0.1–1  $\mu\text{M}$  was slightly different of that in the range 1–5  $\mu\text{M}$  (Figure 1). The ozone concentrations in aqueous solutions were determined by using the indigo method [30]. The color change of the indigo solution was determined by a spectrophotometer (Hach, model DR3900, Loveland, CO, USA). The pH of aqueous solutions was measured by a pH meter (Jenway, model 3540, Staffordshire, UK).

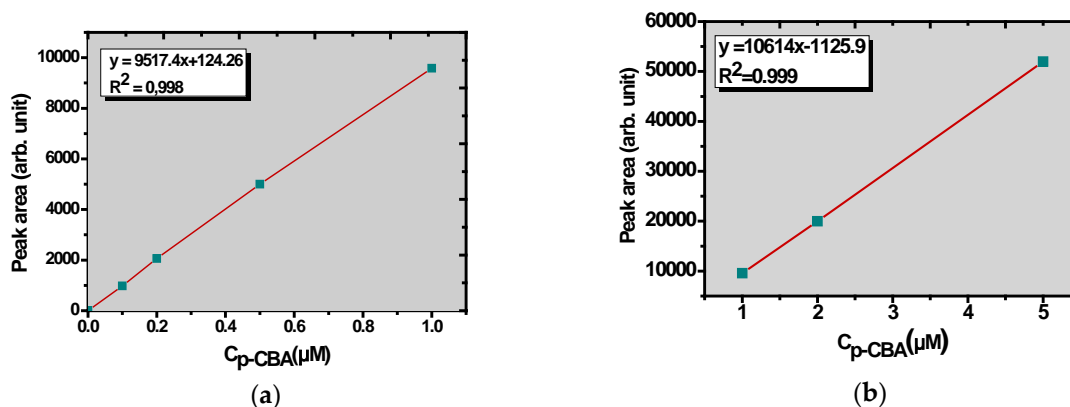


**Figure 1.** p-CBA calibration curves at different concentration ranges; (a) 0–1  $\mu\text{M}$ , and (b) 1–5  $\mu\text{M}$ .

The surface area and the pore size distribution of the modified TMFx catalysts were calculated according to the Brunauer-Emmet-Teller (BET) method. The morphologies of hydrophobically modified TMFx catalysts were examined by scanning electron microscopy (SEM, JEOL model JSM-6390LV, Peabody, MA, USA). PZC and surface charge density were determined by the potentiometric mass titration method [31].

### 3. Results

The affinity/adsorption of p-CBA against the applied catalysts was evaluated through their adsorption capacity. After that the degradation/removal of p-CBA by the application of single ozonation, as well as by catalytic ozonation using the hydrophilic TMFx, the hydrophobically modified TMFx and the hydrophobic PET were also investigated.

#### 3.1. Characterization of the Hydrophobically Modified TMFx

Figure 2 presents the scanning electron microscopy (SEM) image of hydrophobically modified TMFx-50 nanoparticles, noting however that the SEM analysis of examined catalysts' surface showed that all the modified catalysts presents the same (more or less) morphology. The respective elemental analysis (Table 2) revealed that the Si concentration of TMFx-10, TMFx-50, TMFx-100 and TMFx-250 was lower than the applied method's detection limit (0.5 wt %), whereas the Si concentration of TMFx-500 and TMFx-1000 was 0.5 wt % and 1.5 wt %, respectively. The results of Si concentrations (Table 2) were obtained from the average values of the indicating five spectrum areas (Figure 2). Furthermore, the applied hydrophobic modification was not found to significantly change the surface charge density, while there was a slightly decreased surface area of the modified TMFx catalysts in comparison with the (original) hydrophilic one. Table 2 summarizes the aforementioned major physicochemical characteristics of TMFx catalysts. It seems that the only substantial difference between the prepared six modified catalysts was the measured Si concentration onto their surface, which is the main factor expected to affect their wettability (or hydrophobicity).

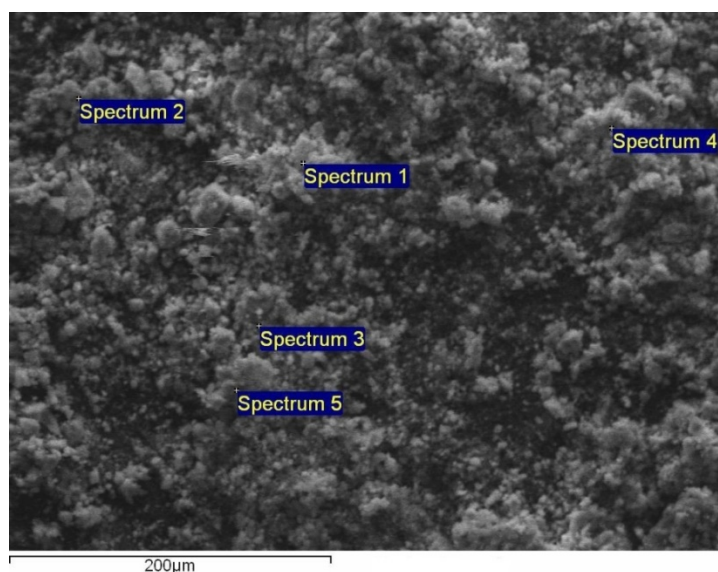


Figure 2. Representative SEM micrograph of TMFx-50 catalyst.

Table 2. Major physicochemical characteristics of modified TMFx catalysts.

Characteristics	Fe/Mn (wt %)	Si (wt %)	PZC	Surface Charge (mmol OH <sup>-</sup> /g)	Surface Charge (mmol H <sup>+</sup> /g)	S <sub>BET</sub> (m <sup>2</sup> /g)	Pore Volume (mL/g)
TMFx	41/12.7	0	3.4	3.24	0.13	85	0.12
TMFx-10	41/12.7	0	3.05	3.32	0.10	60.4	0.45
TMFx-50	41/12.7	<0.5	3.05	3.36	0.10	63.5	0.43
TMFx-100	41/12.7	<0.5	3.05	3.37	0.16	62.7	0.46
TMFx-250	41/12.7	<0.5	3.05	3.40	0.27	67.6	0.52
TMFx-500	41/12.7	0.5	3.05	3.44	0.27	63.3	0.41
TMFx-1000	41/12.7	1.5	3.05	3.37	0.27	60.0	0.47

### 3.2. Adsorption of p-CBA by the Examined Catalysts

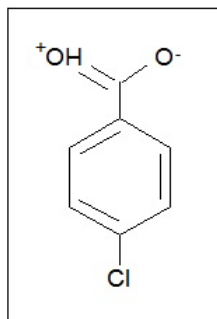
The adsorption of p-CBA from aqueous solution by the examined catalysts (TMFx samples and PET) showed rather low uptake capacity at pH 7 (Tables 3 and 4). TMFx catalysts showed significantly higher uptake capacity than PET, with TMFx-50 to present the relatively higher value (250 μg p-CBA/g), although it has not the higher pore volume. The adsorption capacity strongly depends on surface charge density of adsorbent. Therefore, the adsorption capacity of p-CBA mainly depends on positive charge density of TMFx, which is not modified by hydrophobicity process (Table 2). In contrast, a significant increase of negative charge density was observed by increasing TriClMS from 50 mg/L (0.1 mmol H<sup>+</sup>/g) to 250 mg/L (0.27 mmol H<sup>+</sup>/g) resulting in repulsing of positively charged p-CBA and diminishing thus adsorption capacity. Figure 3 presents p-CBA molecule (pK<sub>a</sub> = 3.99) in ionization equilibrium. When the pH of the solution is lower than pK<sub>a</sub>, p-CBA is in protonated form, while at pH 7 (experimental condition) the molecule is negatively charged (deprotonated form). Furthermore, 50 mg/L concentration of TriClMS can significantly modify the hydrophobicity of TMFx, while preserving simultaneously the availability of adsorption sites, which however gradually covered by the increasingly applied TriClMS concentrations, resulting in turn in lower p-CBA uptake capacity. In the case of PET, the higher adsorption capacity (28 μg p-CBA/g) was determined for the lower catalyst concentration 0.5 g/L.

Table 3. Adsorption loading of p-CBA (C<sub>0</sub> = 4 μM) onto the TMFx catalysts (C<sub>TMFx</sub> = 0.5 mg/L).

Parameter	TMFx	TMFx-10	TMFx-50	TMFx-100	TMFx-250	TMFx-500	TMFx-1000
q (μg p-CBA/g TMFx)	125	125	250	167	160	167	136

**Table 4.** Adsorption loading of p-CBA ( $C_0 = 4 \mu\text{M}$ ) on different initial concentrations of PET catalyst.

Parameter (g/L)	0.5	1	2.5	5	10
$q$ ( $\mu\text{g p-CBA/g PET}$ )	28	16	7	7	4



**Figure 3.** Charge of p-CBA in ionization equilibrium.

### 3.3. Catalytic Ozonation with TMFx

Among the objectives of this study was the evaluation of catalyst wettability (hydrophobic-hydrophilic character) for the efficient production of hydroxyl radicals. Therefore, the raw hydrophilic TMFx catalyst, as well as the samples obtained after the hydrophobic modification with TriCIMS [28], were examined. This objective was indirectly estimated by measuring the kinetics of (rapid) ozone decomposition, which gradually increases in relation to the TriCIMS concentration, used for the hydrophobic modification of TMFx (Figure 4). The change of catalyst wettability is considered to be an important factor, due to the fact that ozone is fundamentally a hydrophobic compound, i.e., a property that can result to better affinity/interaction with a hydrophobic catalyst surface.

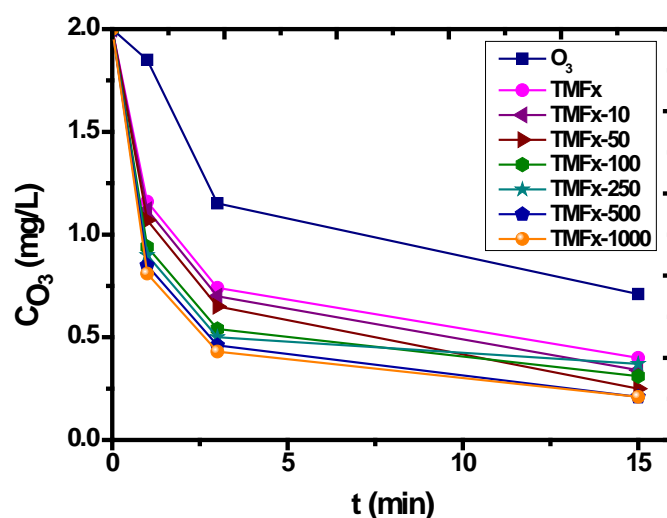


**Figure 4.** Influence of TMFx increased hydrophobicity to ozone decomposition in comparison to single ozonation; experimental conditions:  $C_{O_3} = 2 \text{ mg/L}$ ,  $C_{\text{TMFx}} = 0.5 \text{ g/L}$ ,  $C_{\text{p-CBA}} = 4 \mu\text{M}$ ,  $\text{pH} = 7$ ,  $T = 20 \text{ }^\circ\text{C}$ .

It can be noticed that the increase of used TriCIMS concentration can lead to higher Si concentration on the surface of the catalyst, hence helping to improve the hydrophobic character of the respective catalyst; e.g., TMFx-1000 showed higher ozone decomposition rate, which should probably be attributed to its higher hydrophobicity, enhancing the affinity with ozone.

Considering the degradation of p-CBA, the presence of TMF<sub>x</sub> improved the process efficiency in comparison with the case of single ozonation (Figure 5). Furthermore, the raw (hydrophilic) TMF<sub>x</sub> catalyst showed lower degradation rate of p-CBA, as compared to the modified (hydrophobic) ones, which in turn indicates that the hydrophobic modification of this material has enhanced the production of hydroxyl radicals. After the 3rd min of contact time the degradation efficiency of p-CBA for all the examined modified catalysts passed 95%, while the most efficient catalyst proved to be TMF<sub>x</sub>-50, achieving a degradation rate close to 99% after 15 min ozonation contact time. Based on the data of ozone decomposition rate (Figure 4) it was expected that the best degradation efficiency should be achieved by TMF<sub>x</sub>-1000. However, the degradation of p-CBA can be related better with the data of Table 2, indicating that the pollutant approximation to catalyst surface, i.e., the adsorption efficiency, is the limiting rate step of catalytic ozonation and not simply the hydrophobic character. Table 2 shows that TMF<sub>x</sub>-50 presents the higher adsorption capacity (250 μg p-CBA/g), which means that more p-CBA molecules were adsorbed onto the catalyst surface and thus, they can be easier targeted and effectively degraded by the produced hydroxyl radicals. The application of higher TMF<sub>x</sub> concentrations, although increased the surface hydrophobicity, at the same time seem to consume more active adsorption sites, therefore actually hindering the adsorption of pollutant onto the catalyst surface.

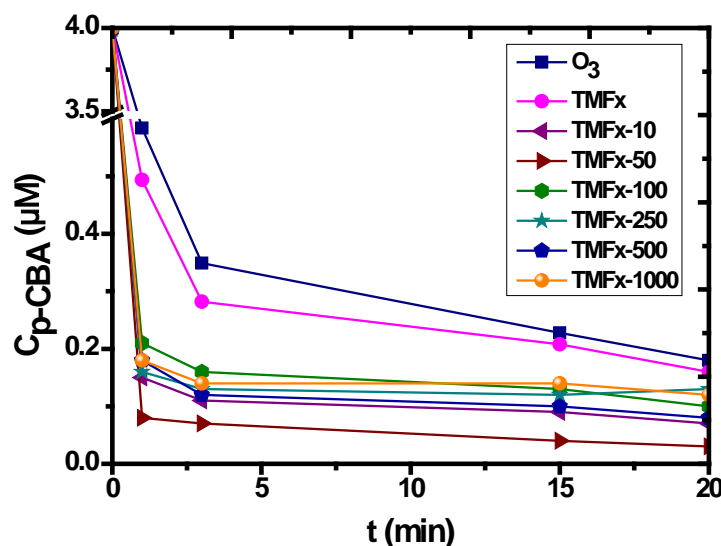


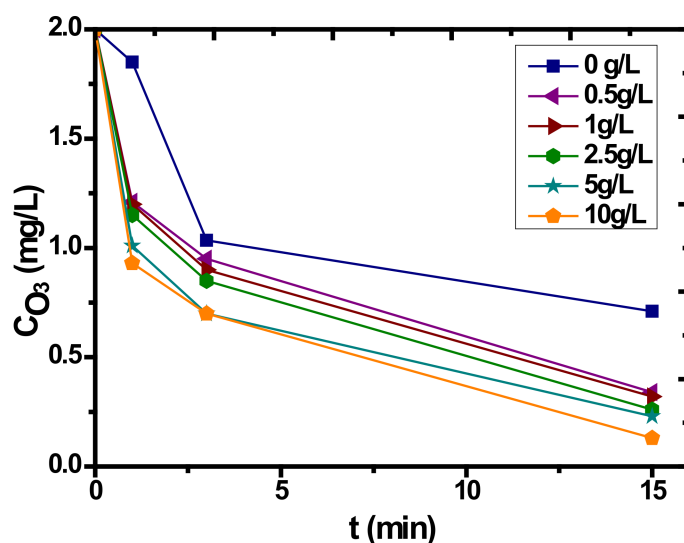
**Figure 5.** Influence of TMF<sub>x</sub> hydrophobicity to p-CBA degradation in comparison with the single ozonation process; experimental conditions: C<sub>O<sub>3</sub></sub> = 2 mg/L, C<sub>TMF<sub>x</sub></sub> = 0.5 g/L, C<sub>p-CBA</sub> = 4 μM, pH = 7, T = 20 °C.

### 3.4. Catalytic Ozonation with PET

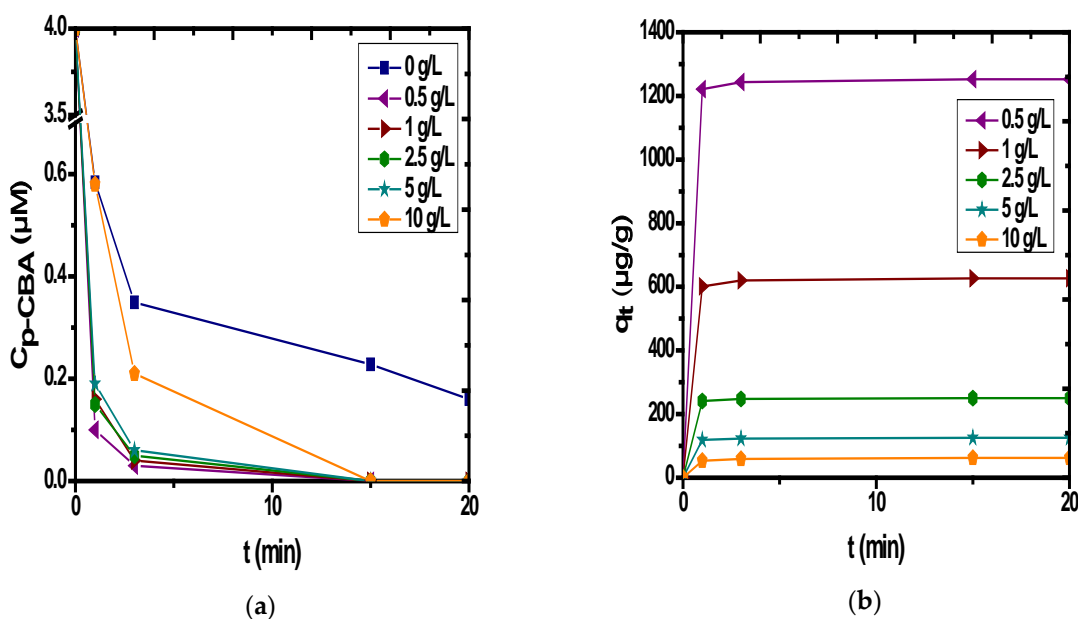
Another important factor influencing the efficient production of hydroxyl radicals is the catalyst dosage. In the case of TMF<sub>x</sub> catalysts the dose was fixed at 0.5 g/L to clarify the influence of “hydrophobicity” factor on the p-CBA adsorption efficiency and its subsequent degradation by ozonation. In the case of PET, which is a natural hydrophobic material, the respective experiments of catalytic ozonation were focused on the influence of adsorption capacity of p-CBA, as obtained by using different initial catalyst concentrations (0.5–10 g/L).

Figure 6 shows the results of ozone decomposition during the catalytic ozonation, when using PET as catalyst. The increase of PET concentrations in the process was found to increase the decomposition of ozone almost proportionally with the catalyst concentration; however, the micro-pollutant removal was not showed the same behavior. From the results presented in Figure 7a it is obvious that the highest degradation was occurred when the PET concentration was 0.5 g/L, which can achieve up to 97.5% p-CBA removal already after the 1st min of reaction/ozonation time. However, for all the

examined catalyst concentrations, (almost) complete degradation of p-CBA (i.e., close to the respective analytical detection limit) was achieved after 15 min reaction time.



**Figure 6.** Influence of PET dosage in the decomposition of ozone during the heterogeneous catalytic ozonation of p-CBA; experimental conditions:  $C_{O_3} = 2 \text{ mg/L}$ ,  $C_{p-CBA} = 4 \text{ }\mu\text{M}$ ,  $\text{pH} = 7$ ,  $T = 20 \text{ }^\circ\text{C}$ .



**Figure 7.** Influence of PET dosage on removal of p-CBA during the heterogeneous catalytic ozonation; (a) Removal of p-CBA ( $\mu\text{M}$ ), (b) Removal of p-CBA expressed as  $\mu\text{g/g}$  catalyst; experimental conditions:  $C_{O_3} = 2 \text{ mg/L}$ ,  $C_{p-CBA} = 4 \text{ }\mu\text{M}$ ,  $\text{pH} = 7$ ,  $T = 20 \text{ }^\circ\text{C}$ .

Although ozone decomposition was found to increase with the catalyst concentration, due to the increase of active catalyst sites, this was not found to enhance the degradation of p-CBA respectively. Figure 7b shows the removal of p-CBA ( $\mu\text{g/g}$  of catalyst) with the reaction/contact time. When 0.5 g/L PET was added to the system, p-CBA was degraded faster, as the slope of the line between 0 and 1 min is greater than in all other examined cases; the increase of PET concentration decreases the kinetics of p-CBA removal.

A possible explanation for the better efficiency obtained by the lower (0.5 g/L PET) dosage is the higher adsorption capacity, observed in this case (28  $\mu\text{g}$  p-CBA/g catalyst), which can be attributed to the following:

- The p-CBA can cover greater percentage of active PET sites, enhancing its degradation rate of this organic compound.
- Simultaneously, by increasing the PET dosage, the free active sites are proportionally increased, resulting in enhanced ozone decomposition and lower  $\text{OH}\cdot$  production, even without the presence of p-CBA.

#### 4. Discussion

The mechanisms of heterogeneous catalytic ozonation process are not clear and there are several explanations in the literature. However, there are three main possible mechanisms:

- Chemisorption of ozone onto the catalyst surface and further reaction with the free (non-sorbed) organic molecules.
- Chemisorption of the organic molecules on the surface of the catalyst and reaction with aqueous (dissolved) or gaseous ozone.
- Chemisorption of both organic molecule and ozone onto the catalyst surface and further reaction between them.

Two of these mechanisms consider the preliminary adsorption process of the organic compounds to be oxidized/removed onto the catalyst surface as the main treatment controlling step [5]. Also, several published papers have showed the important role of adsorption during this treatment process [11,32,33].

The assessment of catalyst concentration on the efficiency of catalytic ozonation reveals that the increase (in this case) of PET concentration in the treatment system was not found to improve the ozonation efficiency, as illustrated in Figure 7. However, ozone decomposition increased with catalyst concentration the optimum concentration for p-CBA removal was achieved by the smaller concentration of PET (0.5 g /L), because in this case the adsorption capacity of the catalyst was higher (Table 4), resulting in greater covering of active sites, and thus, enhancing the degradation rate of p-CBA, due to the easier targeting of adsorbed pollutant molecules during the subsequent ozonation process.

Similar results were observed also for the case of TMFx catalysts. The aqueous ozone decomposition study (Figure 4) indicates that although higher ozone decomposition rates were observed during the catalytic process for the case of TMFx-1000 catalyst, still there was a lack of catalytic activity, regarding the subsequent ozonation. The highest catalytic removal (Figure 5) was observed when TMFx-50 was added in the system, showing the highest adsorption capacity (250  $\mu\text{g}$  of p-CBA/g catalyst) among all the other examined TMFx materials.

Comparison of these results with the relevant publications indicates the crucial role of adsorption capacity, played in the catalytic ozonation process. In addition, except for the initial hydrophilic TMFx, all the other TMFx samples, which were hydrophobically modified, were found capable of accelerating the production of hydroxyl radicals.

At this stage, it is difficult to propose a mechanism for the reactions that are taking place for the removal of p-CBA. Further experiments are needed to explore the mechanism of catalytic ozonation on TMFx and PET. Generally, as mentioned before, the adsorption of ozone or/and organic molecule on catalyst surface favors catalytic ozonation. Ozone can attack micropollutants directly or indirectly through the production of hydroxyl radicals. The production of these oxidative species depends on the water matrix (pH, alkalinity, organic matter (NOM)) [6]. All the experiments were carried out at pH 7 and distilled water. As previously mentioned, the target compound (p-CBA) is considered to be an  $\text{OH}\cdot$  probe compound, because it reacts quickly with the hydroxyl radicals ( $k_{\text{OH}\cdot/\text{p-CBA}} = 5 \times 10^9 \text{ M}^{-1}\text{s}^{-1}$ ) and at the same time presents very low reactivity against ozone

molecules ( $k_{O_3/p-CBA} < 0.15 \text{ M}^{-1}\text{s}^{-1}$ ) [22,23]. This means that p-CBA was degraded only by hydroxyl radicals. The combination of these results may indicate that part of the ozone decomposition proceeds through hydroxyl radical formation even without the addition of a catalyst. However, the hydrophobic catalysts attract ozone, which is a non-polar molecule, thus facilitating ozone approximation to solid surface. The acceleration of ozone decomposition in the cases of hydrophobic modified TMFx and PET indicates that ozone decomposition takes place on the active centers of the catalyst surface, which favors the formation of hydroxyl radicals. Consequently, the adsorption of p-CBA on the catalyst surface can be assumed as an important stage at catalytic ozonation process. Therefore, although it is not fully supported by the experimental results, the mechanism of catalytic ozonation in both cases (TMFx and PET) seems to proceed via the adsorption of p-CBA onto and its attack by the hydroxyl radicals formed onto catalyst surface.

In Figure 8, the efficiencies of single ozonation, TMFx-50 and PET are compared, showing that at 15 min reaction/ozonation time the removal of p-CBA was 96%, 98.7% and (almost) 100% respectively. These results justify the proposed mechanism, i.e., the existence of a synergistic effect between ozonation and adsorption along with the contribution of hydrophobicity in hydroxyl radical formation onto catalyst surface.

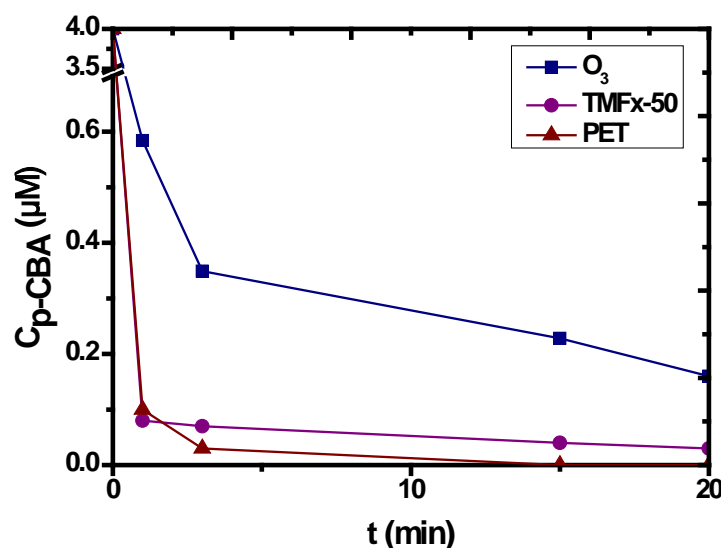


**Figure 8.** Catalytic ozonation with TMFx-50 and PET catalysts in comparison to single ozonation; experimental conditions:  $C_{O_3} = 2 \text{ mg/L}$ ,  $C_{TMFx} = 0.5 \text{ g/L}$ ,  $C_{PET} = 0.5 \text{ g/L}$ ,  $C_{p-CBA} = 4 \text{ μM}$ ,  $\text{pH} = 7$ ,  $T = 20 \text{ °C}$ .

## 5. Conclusions

The heterogeneous catalytic ozonation of p-CBA by using TMFx and PET as catalysts in aqueous solutions was found to be capable for the increased removal/degradation of initial p-CBA concentration, more than in the case of using the single ozonation process application. Since the p-CBA degradation is particularly favored by the presence of hydroxyl radicals (and not by single ozonation) it is concluded that all the examined catalysts can enhance the decomposition of ozone on their reactive sites. Best results were obtained with the presence of PET at 15 min reaction time with p-CBA removal almost 100% for all the examined PET concentrations (0.5–10 g/L); however, the optimum dosage was 0.5 g/L, with 97.5% p-CBA removal noticed already from the 1st reaction min. The hydrophobic modification of TMFx material was found to improve the removal of p-CBA. All modified TMFx samples present similar physicochemical characteristics and consequently similar performance; however, the best results, i.e., 98.7% p-CBA removal after 15 min reaction time, were obtained with the application of TMFx-50 as catalyst. The optimum results for both TMFx and PET materials are related

to the better adsorption capacity of p-CBA, which indicates the vital role of preliminary adsorption in the heterogeneous catalytic ozonation process.

**Author Contributions:** Conceptualization, S.P., A.Z. and M.M.; Methodology, S.S.; Validation, S.P., A.Z. and M.M.; Investigation, S.P.; Resources, A.Z. and M.M.; Data Curation, S.P.; Writing-Original Draft Preparation, S.P.; Writing-Review & Editing, A.Z.; M.M. and S.S. Visualization, S.P.; Supervision, A.Z. and M.M.; Project Administration, A.Z.

**Funding:** This research received no external funding.

**Conflicts of Interest:** The authors declare no conflict of interest.

## References

1. Brausch, J.M.; Rand, G.M. A review of personal care products in the aquatic environment: Environmental concentrations and toxicity. *Chemosphere* **2011**, *82*, 1518–1532. [[CrossRef](#)] [[PubMed](#)]
2. Sauv e, S.; Desrosiers, M. A review of what is an emerging contaminant. *Chem. Cent. J.* **2014**, *8*. [[CrossRef](#)] [[PubMed](#)]
3. Klavarioti, M.; Mantzavinos, D.; Kassinos, D. Removal of residual pharmaceuticals from aqueous systems by advanced oxidation processes. *Environ. Int.* **2009**, *35*, 402–417. [[CrossRef](#)] [[PubMed](#)]
4. Ikehata, K.; Jodeiri Naghashkar, N.; Gamal El-Din, M. Degradation of aqueous pharmaceuticals by ozonation and advanced oxidation processes: A review. *Ozone Sci. Eng.* **2006**, *28*, 353–414. [[CrossRef](#)]
5. Kasprzyk-Hordern, B.; Zi olek, M.; Nawrocki, J. Catalytic ozonation and methods of enhancing molecular ozone reactions in water treatment. *Appl. Catal. B Environ.* **2003**, *46*, 639–669. [[CrossRef](#)]
6. Von Gunten, U. Ozonation of drinking water: Part I. Oxidation kinetics and product formation. *Water Res.* **2003**, *37*, 1443–1467. [[CrossRef](#)]
7. Nawrocki, J. Catalytic ozonation in water: Controversies and questions. Discussion paper. *Appl. Catal. B Environ.* **2013**, *142–143*, 465–471. [[CrossRef](#)]
8. Andreozzi, R. Advanced oxidation processes (AOP) for water purification and recovery. *Catal. Today* **1999**, *53*, 51–59. [[CrossRef](#)]
9. Martins, R.C.; Quinta-Ferreira, R.M. Catalytic ozonation of phenolic acids over a Mn-Ce-O catalyst. *Appl. Catal. B Environ.* **2009**, *90*, 268–277. [[CrossRef](#)]
10. Ma, J.; Sui, M.; Zhang, T.; Guan, C. Effect of pH on MnOx/GAC catalyzed ozonation for degradation of nitrobenzene. *Water Res.* **2005**, *39*, 779–786. [[CrossRef](#)] [[PubMed](#)]
11. Rosal, R.; Rodr guez, A.; Gonzalo, M.S.; Garc a-Calvo, E. Catalytic ozonation of naproxen and carbamazepine on titanium dioxide. *Appl. Catal. B Environ.* **2008**, *84*, 48–57. [[CrossRef](#)]
12. Tong, S.P.; Liu, W.P.; Leng, W.H.; Zhang, Q.Q. Characteristics of MnO<sub>2</sub> catalytic ozonation of sulfosalicylic acid and propionic acid in water. *Chemosphere* **2003**, *50*, 1359–1364. [[CrossRef](#)]
13. Amutha, R.; Sillanp a, M.; Lee, G.J.; Lin, J.C.; Yang, C.K.; Wu, J.J. Catalytic ozonation of 2-ethoxy ethyl acetate using mesoporous nickel oxalates. *Catal. Commun.* **2014**, *43*, 88–92. [[CrossRef](#)]
14. Sui, M.; Sheng, L.; Lu, K.; Tian, F. FeOOH catalytic ozonation of oxalic acid and the effect of phosphate binding on its catalytic activity. *Appl. Catal. B Environ.* **2010**, *96*, 94–100. [[CrossRef](#)]
15. He, K.; Dong, Y.M.; Li, Z.; Yin, L.; Zhang, A.M.; Zheng, Y.C. Catalytic ozonation of phenol in water with natural brucite and magnesite. *J. Hazard. Mater.* **2008**, *159*, 587–592. [[CrossRef](#)] [[PubMed](#)]
16. Guzman-Perez, C.A.; Soltan, J.; Robertson, J. Kinetics of catalytic ozonation of atrazine in the presence of activated carbon. *Sep. Purif. Technol.* **2011**, *79*, 8–14. [[CrossRef](#)]
17. Vald s, H.; Murillo, F.A.; Manoli, J.A.; Zaror, C.A. Heterogeneous catalytic ozonation of benzothiazole aqueous solution promoted by volcanic sand. *J. Hazard. Mater.* **2008**, *153*, 1036–1042. [[CrossRef](#)] [[PubMed](#)]
18. Dong, Y.; He, K.; Zhao, B.; Yin, Y.; Yin, L.; Zhang, A. Catalytic ozonation of azo dye active brilliant red X-3B in water with natural mineral brucite. *Catal. Commun.* **2007**, *8*, 1599–1603. [[CrossRef](#)]
19. Ma, J.; Chen, Y.; Nie, J.; Ma, L.; Huang, Y.; Li, L.; Liu, Y.; Guo, Z. Pilot-scale study on catalytic ozonation of bio-treated dyeing and finishing wastewater using recycled waste iron shavings as a catalyst. *Sci. Rep.* **2018**, *8*, 7555. [[CrossRef](#)] [[PubMed](#)]
20. Niedan, V.; Scholer, H.F. Natural Formation of Chlorobenzoic Acids (CBA) and Distinction between PCB-Degraded CBA. *Science* **1997**, *35*, 1233–1241. [[CrossRef](#)]

21. Han, W.; Zhang, P.; Zhu, W.; Yin, J.; Li, L. Photocatalysis of p-chlorobenzoic acid in aqueous solution under irradiation of 254 nm and 185 nm UV light. *Water Res.* **2004**, *38*, 4197–4203. [[CrossRef](#)] [[PubMed](#)]
22. Elovitz, M.S.; von Gunten, U. Hydroxyl Radical/Ozone Ratios during Ozonation Processes. I. The  $R_{ct}$  Concept. *Ozone Sci. Eng.* **1999**, *21*, 239–260. [[CrossRef](#)]
23. Pi, Y.; Schumacher, J.; Jekel, M. The use of para-chlorobenzoic acid (pCBA) as an ozone/hydroxyl radical probe compound. *Ozone Sci. Eng.* **2005**, *27*, 431–436. [[CrossRef](#)]
24. Centurião, A.P.S.L.; Baldissarelli, V.Z.; Scaratti, G.; de Amorim, M.S.; Moreira, R.F.P.M. Enhanced ozonation degradation of petroleum refinery wastewater in the presence of oxide nanocatalysts. *Environ. Technol.* **2018**, *1*–11. [[CrossRef](#)] [[PubMed](#)]
25. Xing, S.; Lu, X.; Liu, J.; Zhu, L.; Ma, Z.; Wu, Y. Catalytic ozonation of sulfosalicylic acid over manganese oxide supported on mesoporous ceria. *Chemosphere* **2016**, *144*, 7–12. [[CrossRef](#)] [[PubMed](#)]
26. Wang, Y.; Yang, W.; Yin, X.; Liu, Y. The role of Mn-doping for catalytic ozonation of phenol using Mn/ $\gamma$ - $Al_2O_3$  nanocatalyst: Performance and mechanism. *J. Environ. Chem. Eng.* **2016**, *4*, 3415–3425. [[CrossRef](#)]
27. Kokkinos, E.; Simeonidis, K.; Pinakidou, F.; Katsikini, M.; Mitrakas, M. Optimization of tetravalent manganese ferrioxalate's negative charge density: A high-performing mercury adsorbent from drinking water. *Sci. Total Environ.* **2017**, *574*, 482–489. [[CrossRef](#)] [[PubMed](#)]
28. Stylianou, S.K.; Sklari, S.D.; Zamboulis, D.; Zaspalis, V.T.; Zouboulis, A.I. Development of bubble-less ozonation and membrane filtration process for the treatment of contaminated water. *J. Membr. Sci.* **2015**, *492*, 40–47. [[CrossRef](#)]
29. Staehelld, J.; Hoigne, J. Decomposition of Ozone in Water in the Presence of Organic Solutes Acting as Promoters and Inhibitors of Radical Chain Reactions. *Environ. Sci. Technol.* **1985**, *19*, 1206–1213. [[CrossRef](#)] [[PubMed](#)]
30. Clesceri, S.L.; Greenberg, E.A.; Trussell, R.R. Inorganic Nonmetals. In *Standard Methods for Examination of Water and Wastewater*, 17th ed.; American Public Health Association: Washington, DC, USA, 1989; pp. 162–165. ISBN 0-87553-161-X.
31. Kosmulski, M. *Surface Charging and Points Zero Charge*; CRC: Boca Raton, FL, USA, 2009; Volume 145, ISBN 978-1-4200-51889-9.
32. Beltrán, F.J.; Rivas, F.J.; Montero-De-Espinosa, R. A  $TiO_2/Al_2O_3$  catalyst to improve the ozonation of oxalic acid in water. *Appl. Catal. B Environ.* **2004**, *47*, 101–109. [[CrossRef](#)]
33. Faria, P.C.C.; Órfão, J.J.M.; Pereira, M.F.R. Activated carbon catalytic ozonation of oxamic and oxalic acids. *Appl. Catal. B Environ.* **2008**, *79*, 237–243. [[CrossRef](#)]



© 2018 by the authors. Licensee MDPI, Basel, Switzerland. This article is an open access article distributed under the terms and conditions of the Creative Commons Attribution (CC BY) license (<http://creativecommons.org/licenses/by/4.0/>).